REAL-TIME SELECTIVE MONITORING OF EXPOSURE CONTROLLED PROJECTION LITHOGRAPHY

Harrison H. Jones, Abhishek Kwatra, Amit S. Jariwala , David W. Rosen*
George W. Woodruff School of Mechanical Engineering
, Atlanta, Georgia, 30332
*Corresponding author. Tel.: +1 404 894 9668 Email: david.rosen@me.gatech.edu

Abstract:

Exposure Controlled Projection Lithography (ECPL) is a stereolithographic process in which incident radiation, patterned by a dynamic mask, passes through a transparent substrate to cure photopolymer which grows progressively from the substrate surface. We present here a novel method of capturing useful information about the curing process from a simple, inexpensive, real-time monitoring system based on interferometry. This approach can be used to provide feedback control to the ECPL process, thus making the process more robust and increasing system accuracy. The results obtained from this monitoring system provide a means to better visualize and understand the various phenomena occurring during the photo-polymerization of transparent photopolymers. In order to lessen the measurement error, caused by internal diffraction within the substrate, the interferometry system has been designed such that the laser light used can be selectively targeted. This selective monitoring approach is experimentally validated to measure the height and profile of the cured part in real-time.

1. Introduction

Exposure Controlled Projection Lithography (ECPL) is a manufacturing process in which physical objects are produced by selectively masking a projected beam of light onto a bath of photopolymer resin. Lithography processes, such as stereolithography (SLA), traditionally use a scanning curing laser in conjunction with a bath of photopolymer resin to progressively build models layer by layer. After a scanning pass is complete the build platform is dipped into the bath of resin, a thin layer of resin is wiped over the already existing layers, and the platform rises; ready for another laser pass. This process continues until the part is complete. Research regarding the use of a dynamic mask to control the exposure of light onto a photopolymer resin as to manufacture viable three dimensional models has been recently conducted by Limaye & Rosen[1], Sun et al[2], Chatwin[3], Monneret et al. [4], and Jariwala et al. [5]. In their research, a dynamic mask is used in place of the physical beam scan of a traditional SLA process. Commercial lithography machines exist [6] which use a dynamic mask and a layer by layer process to produce physical models. The ECPL process does not however, follow a traditional lithography process. In the ECPL process, radiation is dynamically masked and then projected through a transparent "build platform" into a resin chamber. By altering the dynamic mask's shape and intensity, the 3D shape of the model can be fully defined. A similar process has been a topic of research for Erdmann et all. [7] and Mizukami et all. [8]. Controlling the process to relate 3D part models to the appropriate dynamic masks sequence has been an ongoing research effort.

Jariwala et al. [5] had proposed a processing plan which uses models of the chemical photopolymerization of the resin to estimate the part height given a particular dynamic mask. This model produced rough estimations of final cured part height. Later attempts by Jariwala et al. [10] to expand on this model produced more precise but still rough estimations of part height.

An interferometry-based control system, the Interferometric Curing Monitoring (ICM) system, was then proposed by Jariwala et al. [11] in an attempt to build a more precise ECPL system which utilized control theory to automatically adjust the dynamic mask based on the real-time part development. This paper addresses one of the issues currently found in this system: the presence of phase change signals on the interferogram which indicate part curing occurring outside of the region of exposure. A hypothesis is presented which proposes that internal reflection of the ICM laser light between the two surfaces of the resin chamber might be the cause of this error. A proposed solution for eliminating this error is demonstrated by selectively targeting a small beam of ICM laser.

2. System Overview

2.1 ECPL System

The ECPL system, as illustrated in Figure 1, consists of five core components: the radiation source, the beam conditioning system, the dynamic mask generator, the projection system, and the resin chamber. Curing radiation is passed through the beam conditioning system which homogenizes the light. Next, this uniform light is projected onto the dynamic mask generator which selectively routes the light into the projection system. The projection system focuses the light onto the resin chamber. Finally, the focused light passes through the bottom transparent substrate of the resin chamber into the photopolymer resin. After a brief period of oxygen-inhibition the portions of resin, exposed to radiation, begin to crosslink to form a solid polymer. Additional radiation passes through this solid polymer into the uncured monomer above and crosslinking continues. The dynamic mask and exposure time determine both the shape and height of the part. After exposure is complete the build chamber is removed and washed as to remove all uncured monomer. The cured part is then post-cured in a bath of UV light as to further cross-link the part and strengthen it.

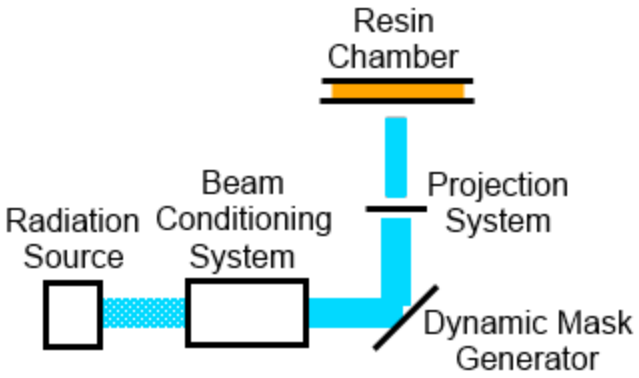

Figure 1 – ECPL System Diagram

Radiation Source:

The radiation source used was an Omnicure S2000 UV spot curing system produced by Lumen Dynamics. This machine was fitted with a 365nm band-pass filter which ensures that it produces UV radiation around 365nm. This wavelength was selected because it the wavelength which initiates crosslinking in the photopolymer. The resulting beam was piped through a light guide to the beam conditioning system.

Beam Conditioning System:

The beam conditioning system consisted of several different diffusers and collimating lenses arranged as to best produce a collimated and homogeneous output. This component is critical to keeping incident radiation on the dynamic mask generator uniform. Non-uniform light is undesirable as it introduces another variable into the system.

Dynamic Mask Generator:

The dynamic mask generator consisted of a Texas Instruments' Digital Micromirror Device (DMD) which is capable of selectively guiding incident radiation in two directions using micromirrors. This device was arranged such that the "ON" state directed the light vertically upwards while the "OFF" state directed the light away from the projection system and resin chamber. The DMD was controlled as a secondary computer monitor using Microsoft PowerPoint Software.

Projection System:

The projection system consisted of a single 0.6x magnifying lens from ThorLabs, Inc. The purpose of the projection system is to focus the incident radiation from the DMD into the resin chamber.

Resin Chamber:

The resin chamber consisted of two glass slides separated by spacers of known thickness. The photopolymer resin was loaded between the two glass slides. This photopolymer resin would crosslink inside this resin chamber, when exposed to UV radiation.

2.2 ICM System

The (ICM) system, as seen in in Figure 2, is based on a Mach-Zehnder interferometer [12] and is described in detail in Jariwala et al. [11]. A coherent laser is directed, through a beam expander, moveable iris, and beam splitter, at the resin chamber. Light reflecting off of the top and bottom surface of the resin chamber's two transparent bounding surfaces reflect through the beam splitter and into the camera. Due to the phase difference between the light coming from the top surface and the light coming from the bottom surface an interference pattern is observed by the camera.

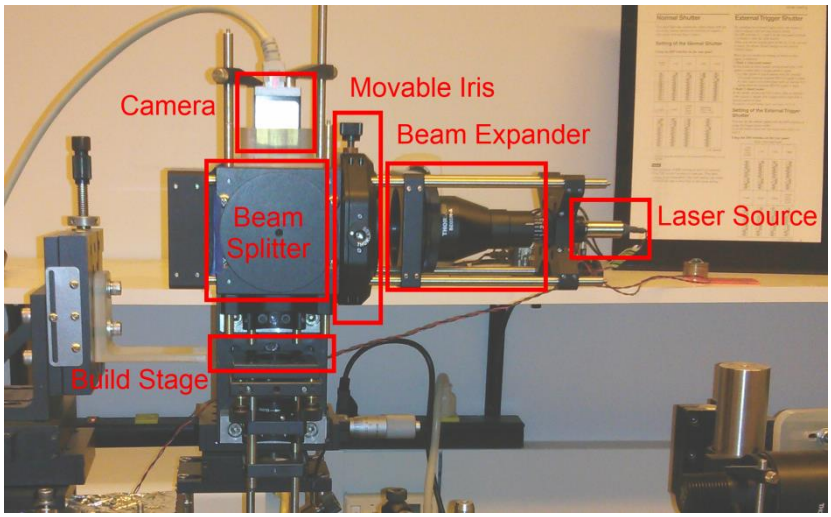

Figure 2 - ICM System

Laser Source

The laser source consisted of a small, lower-power, 670 nm wavelength laser diode. The purpose of this diode was to provide the coherent laser light required for interferometry.

Beam Expander

The purpose of the beam expander was to simply expand the narrow beam produced by the laser source such that the light output is capable of simultaneously bathing the entire resin chamber in light such that any point in the entire curing area can be analyzed by the camera.

Movable Iris

The purpose of the movable iris was twofold: to be able to limit the size of the incident beam and to be able to move that small beam around on the curing plane. This particular function is necessary to validate the hypothesis proposed in this paper. It was used to selectively illuminate a specific location on the curing plane.

2.2.4 Beam Splitter

The purpose of the beam splitter was to reflect laser source downward into the resin chamber while, at the same time, allowing for light coming from the resin chamber to pass through to the camera above.

2.2.5 Camera

The purpose of the camera was to capture the intensity of incoming laser light. As will be shown later, the intensity profile of the resulting laser light shows the interference patters. Tracking this interference pattern over can help calculate the phase shift caused by change in refractive index of the resin curing inside the resin chamber.

3. ICM Working Principle

The ICM system utilizes the principles of interferometry to estimate the height of the part cured in the resin chamber in real time. Referring to Figure 3, the camera records the interferogram produced by the phase difference between the optical paths of the light reflecting from the top surface of the resin chamber and the bottom surface of the resin chamber. The thickness of the resin chamber, t, results in steady state optical path offset which equates to a constant phase shift. The optical path of the light reflecting from the bottom surface is lengthened by the presence of the resin in the resin chamber. The curing process causes the resin to increase density as it crosslinks. This change leads to a longer optical path which results in a slower speed of light. The calculated cured part height can therefore be expressed as a function of the phase shift, or phase oscillation, which is a function of the optical path. As derived in Jariwala et al. [11] the equation for this phase shift is given by:

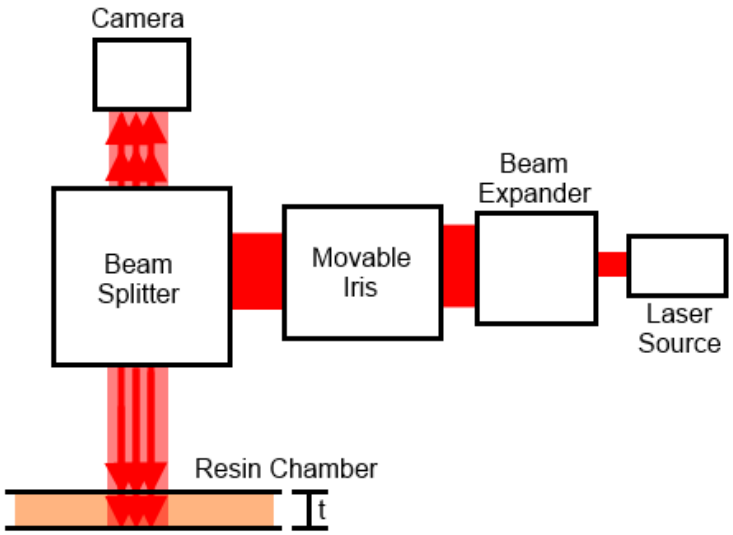

Figure 3 - ICM System Diagram

$$Shift = \frac{2*\Delta n*t}{\lambda} \quad (1)$$

where Δn the change refractive index of resin in the resin chamber, the t is the physical thickness of the cured part in mm, and λ is the laser wavelength in mm. It was experimentally determined in Jariwala et al. [11] that the phase shift is proportional to the cured part height. Thus cured part height could be estimated in real time using the phase shift of the interference pattern captured by the camera.

4. Experimental Procedure

4.1 Preliminary Experiments

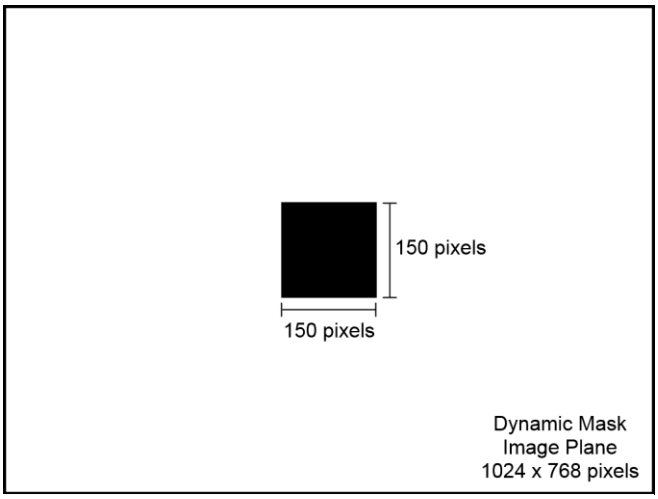

Figure 4 - Black Square on Dynamic Mask Plane

The "standard" procedure followed when using the ICM system to monitor the ECPL process is to bath the entire resin chamber in laser light. To illustrate the effect of monitoring with the entire curing region exposed to the ICM's laser light, the iris was placed in the full open position. In the full open position the beam from the laser through the beam expander covers slightly more than the entire curing region. Next a test part, a 150 pixels by 150 pixels black square bitmap, as seen in Figure 4, was cured by placing the square in the center of the DMD, setting the exposure time to 10 seconds and the UV power level to 22%[1], and then opening the UV shutter. As the shutter was opened a video was taken of the ICM camera's output. In order to fully capture the entire curing process the video was recorded for considerably longer than the exposure time. This was to make sure the effects of "dark cure" as described in Jariwala et al. [11] would be captured in the video.

Analysis of the interferometry video with the iris fully open began with point selection. The video data is then parsed and the intensity of each point on the video is saved. Intensity values are arbitrary as the camera has not been calibrated. A value of 255 intensity is "high" and appears white. A value of 0 intensity is "low" and appears black. Frames are saved ever tenth of a second. A line of ten equidistant points were selected starting from the center of the cured part region. Points one through three were inside the curing region while points five through ten were outside of the curing region. Points one through six were selected for discussion. Point one was in the center of the part and illustrates a typical interferogram. Point three was right on the inside edge of the curing region and was selected to illustrate what the edge of the curing region looks like on an interferogram. Points four, five and six are right outside of the curing region and were selected to illustrate the presence of phase oscillations occurring outside of the curing region. **Error! Reference source not found.** is the last frame of the video recorded by the ICM camera overlaid with the points and their locations. The rectangle represents the approximate location of the curing region.

[1] The power level and exposure time are arbitrary as long as the selected values are high enough to initiate curing.

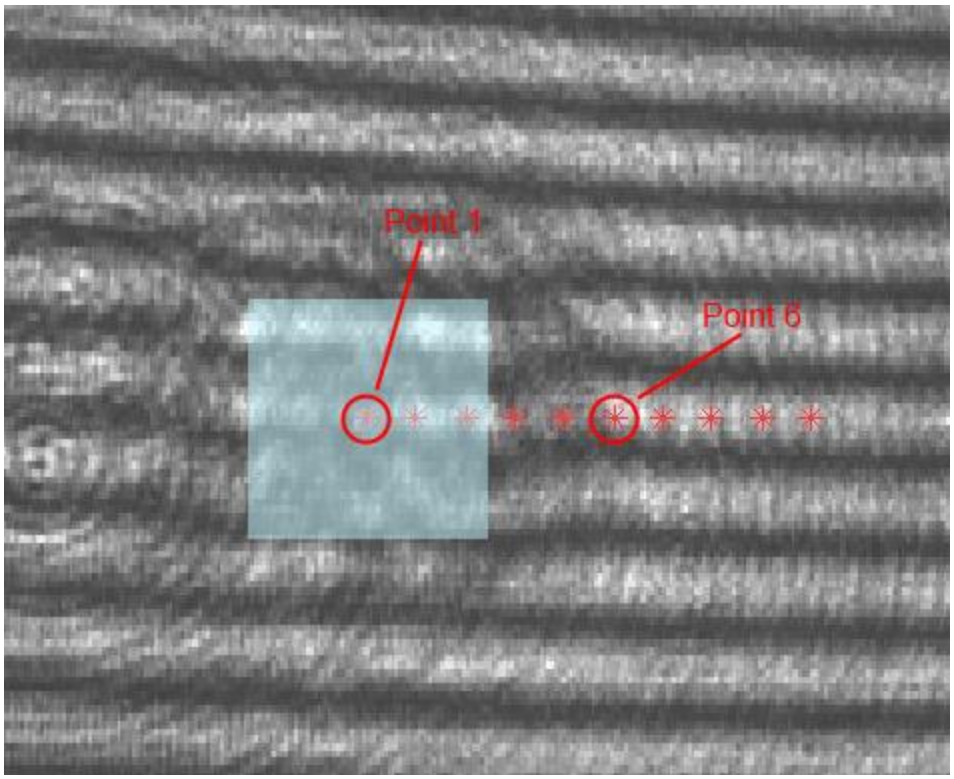

Figure 5 - Points Analyzed, Iris Full Open

Error! Reference source not found. illustrates the phase shift measured each selected point. The presence of phase oscillations at each point suggests that curing occurred at each of these points. This however was not the case. The presentence of phase angle oscillations at points outside of the curing region is the error this paper is addressing.

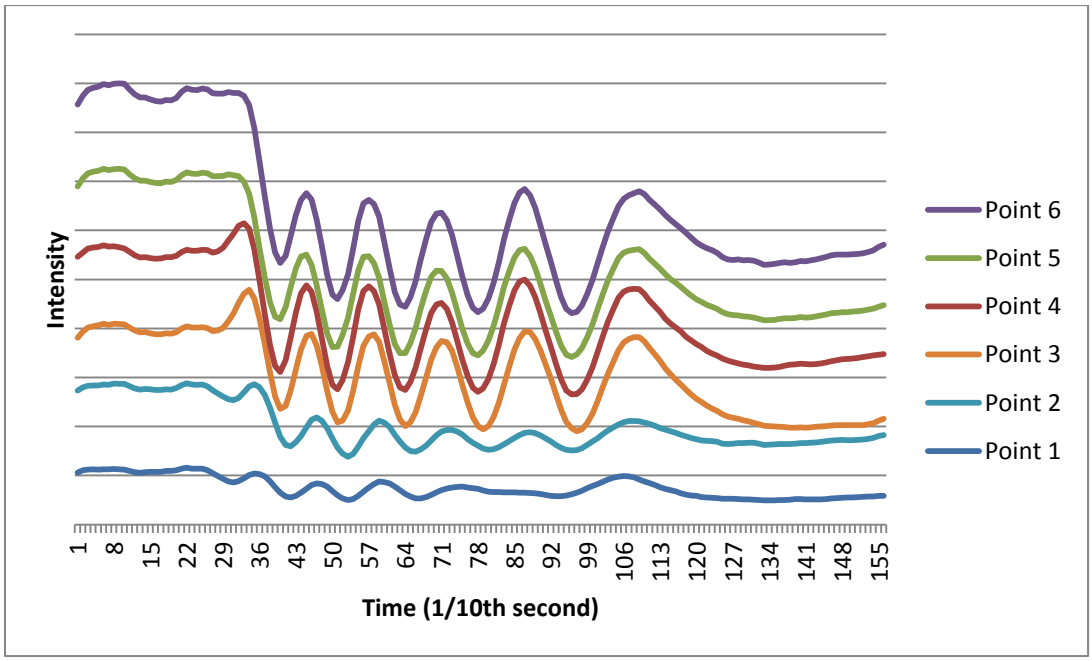

Figure 6 - Selected Points, Iris Fully Open

4.2 Proposed Hypothesis

When using the ICM system with the iris in the full open position, phase oscillations were observed to occur near, but outside of, the curing region. Since phase oscillations should only occur in areas where crosslinking of the monomer was occurring, these oscillations outside of this area were unexpected. The hypothesis for the cause of these unexpected oscillations is that when a beam of light, from the interferometry system, enters the resin chamber some of the light behaves as expected: part of it reflects from the top surface back into the camera and part of it reflects from the bottom surface, through the resin chamber, and then into the camera. However, as illustrated in Figure 7, some of the light reflects internally for a great distance parallel to the curing plane before escaping toward the camera. This would explain why curing phase shift was observed outside the curing region: light which was affected by the curing process was reflecting internally for a short distance, in this case a short distance outside of the curing region, before finally reflecting toward the camera. In order to tests this hypothesis the standard ICM procedure was followed with a few minor changes: the iris was closed to just produce one small beam of light and the iris was moved such that that small beam of light impacted just outside of the curing region. Another follow up experiment placed the beam near the center of the curing region. A 150 pixels by 150 pixels black square was cured using the ECPL process with the identical exposure and UV level parameters. Again, the output of the ICM camera was recorded for sufficient time as to allow "dark cure" to occur.

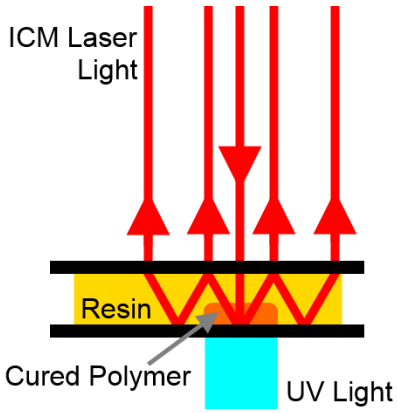

Figure 7 - Internal Light Reflection

5. Results and Discussion

5.2 Experiment Results

Analysis of the interferometry video with the small ICM beam began by selecting the same points used in the preliminary experiment analysis. The video data was then parsed and the intensity of each point on the video was saved. Again, points one through three were inside the curing region while points four through ten were outside of the curing region. Figure 8 and Figure 9 illustrate the points analyzed using the last frame of a video along with a superimposed rectangle to indicate the approximate location of the curing region.

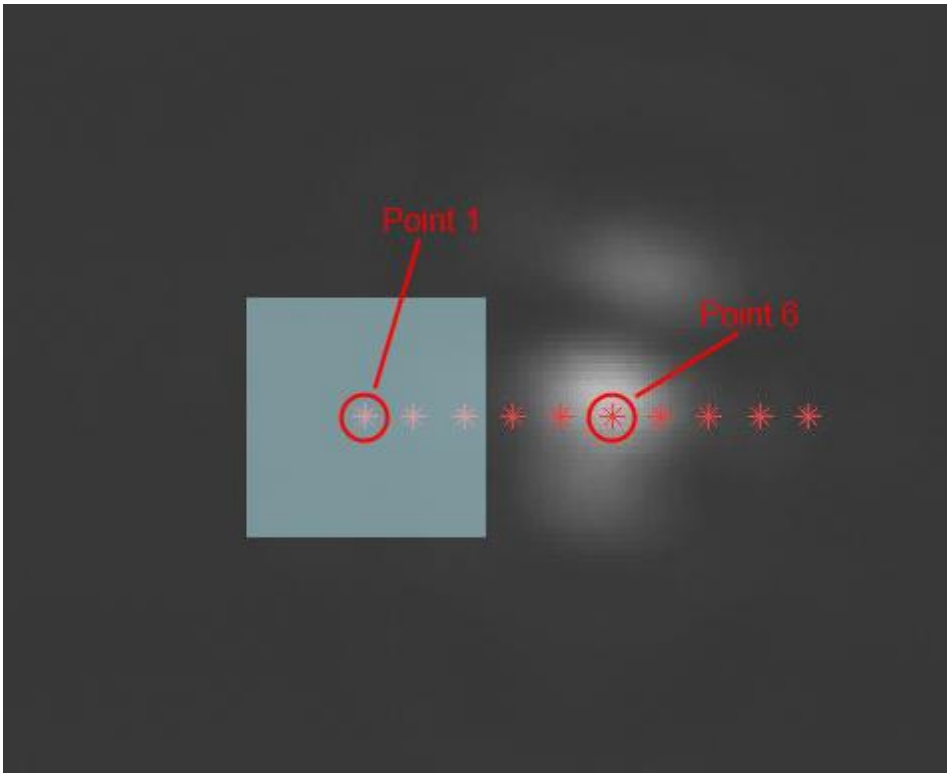

Figure 8 - Points Analyzed, Small Beam Right of Center

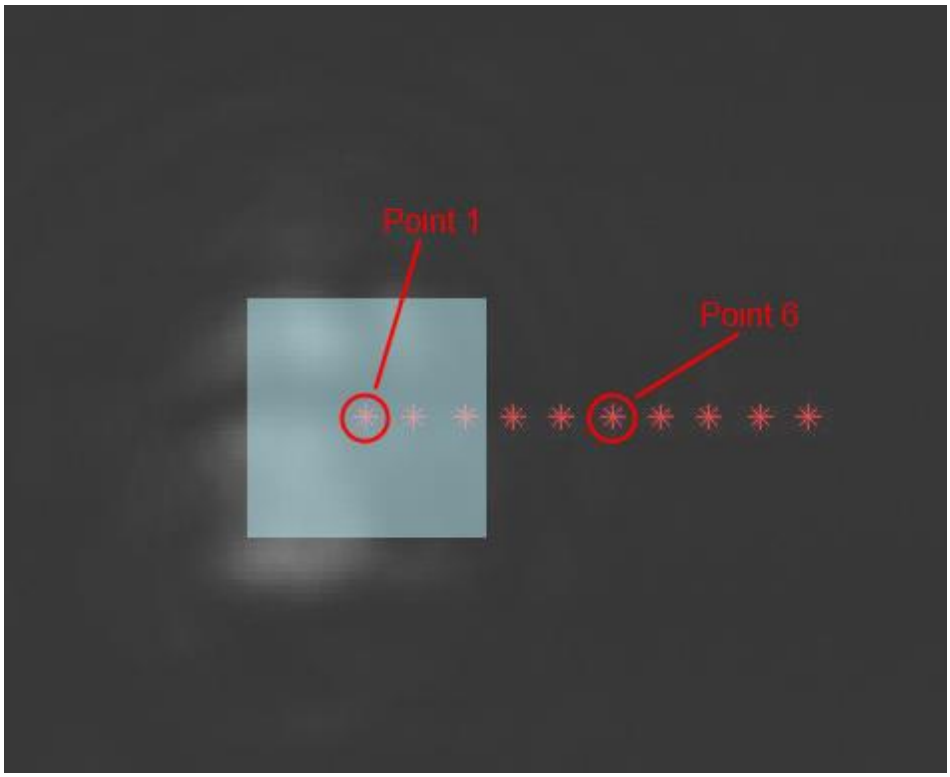

Figure 9 - Points Analyzed, Small Beam Near Center of Part

Figure 10 and Figure 11 illustrate the phase change measured at each analyzed point for the beam off center and near center respectively. Figure 10 shows no phase oscillation at any of the

analyzed points. Since the beam was of small size and off center, the center and edge of the curing region were barely irradiated with the ICM laser. The low intensity levels are not only expected but desired if only the region proximal to the curing region is to be analyzed. Most importantly, points four, five, and six show no phase oscillation as expected given that they are outside of the curing region. When compared to the previous intensity plots of points four, five and six it can be concluded that by restricting the ICM laser to a small point outside of the curing region yields intensity plots with phase change more representative of the level of curing in that location.

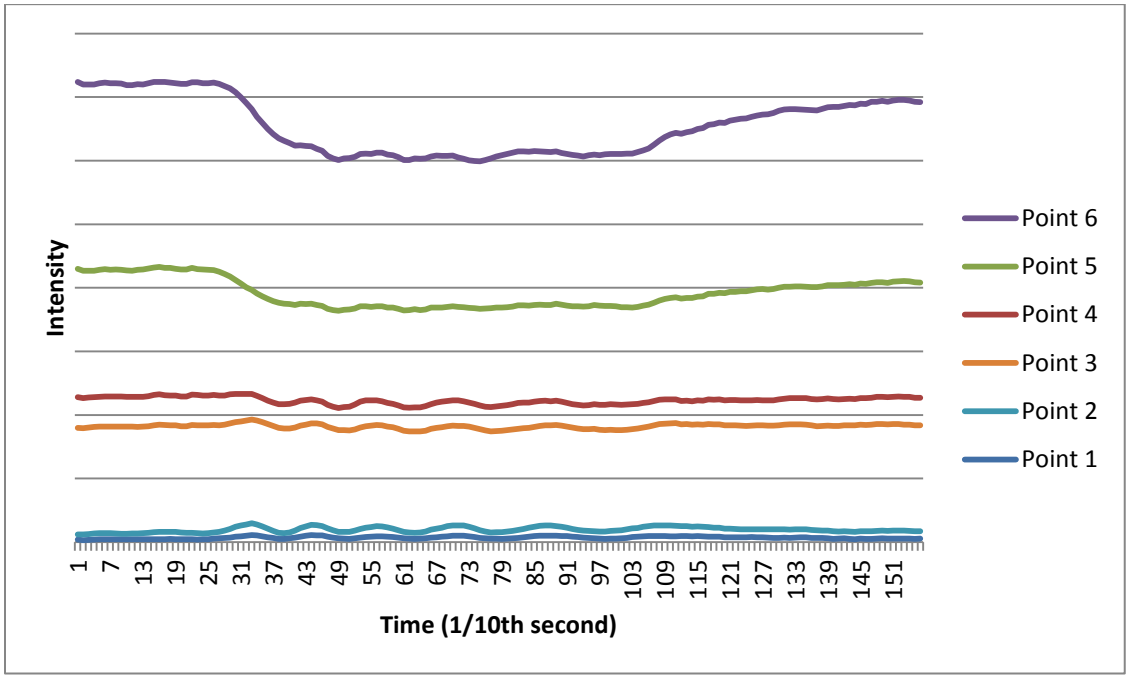

Figure 10 - Selected Points, Beam Right of Center

Figure 11 illustrates that a restricted ICM beam is still capable of capturing the phase oscillations present in the curing region. With the beam centered on the part, points one, two, and three in the curing region show significant phase oscillation while points four, five, and six have little to no phase oscillations as expected for points outside of the curing region. Further investigation is needed to determine if the slight phase oscillations measured at point four and five are a result of the light from the ICM beam bleeding through to other areas outside of the beam or other possible sources of error.

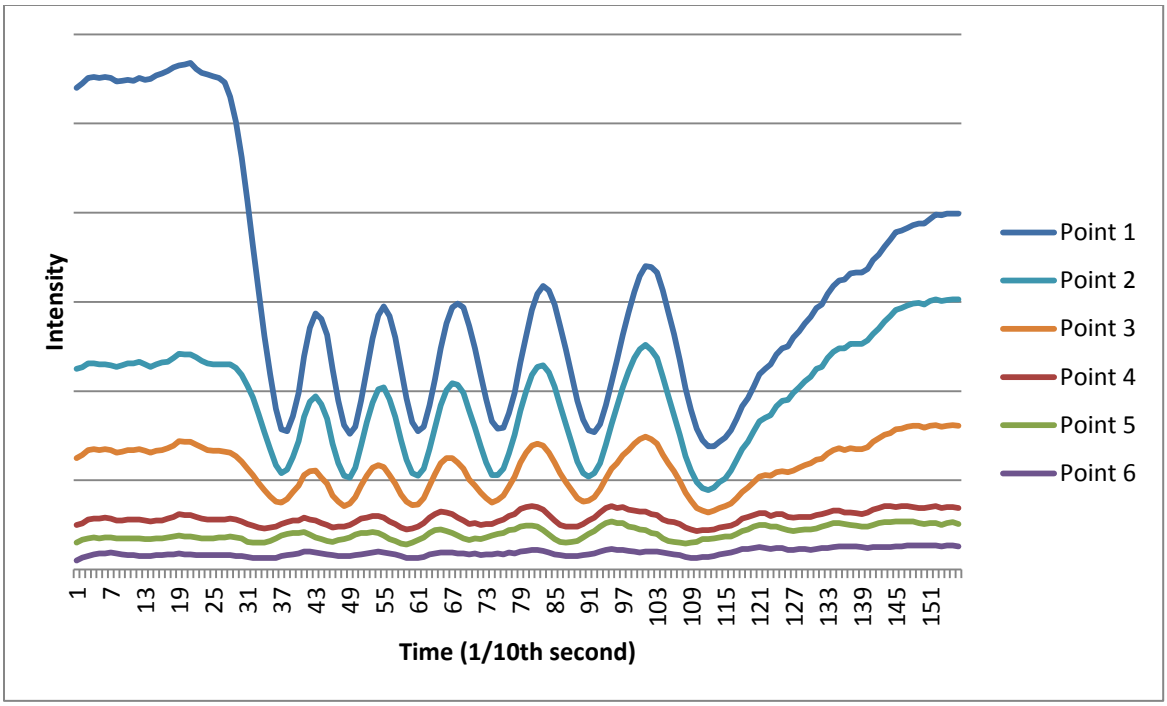

Figure 11 - Selected Points, Beam Centered on Part

6. Conclusions

This paper presented an investigation into the presence of phase oscillations occurring on an interferogram in regions which were not cured. Because phase oscillations indicate part curing, these oscillations are unexpected. By restricting the ICM beam to a small area and then moving that beam to the point to be measured, phase oscillations in uncured areas were greatly diminished or disappeared completely. This result support the hypothesis that internal reflection of ICM laser light caused phase changes to be observed in regions outside of the curing region. If the same region is analyzed with the ICM laser completely bathing the resin chamber, the resulting interferogram will contain phase changes of intensity which indicate curing. By restricting the laser to a small point a more accurate representation of part cure can be obtained.

Because of the difficulty of precisely controlling the beam size and location with the moveable iris, use of a selectively transmissive light modulator, such as a spatial light modulator (SLM), would allow for repeated beam sizes to be selectively and accurately placed. This would allow for the beam to be scanned over the curing region. Such scanning would allow for areas of the curing region to be analyzed by the ICM system as discrete regions with limited interference from internal reflections.

7. Acknowledgements

This material is based upon work supported by the National Science Foundation under Grant No. CMMI-1234561.

8. References

[1] Limaye A. and Rosen D., 2007, “Process Planning Method for Mask Projection Micro-Stereolithography”, *Rapid Prototyping Journal,* **13**(2), pp. 76-84

[2] Sun C., Fang N., Wu D.M., Zhang X., 2005, "Projection Micro-Stereolithography Using Digital Micro-Mirror Dynamic Mask", *Sensors and Actuators A,* **121**, pp. 113-120.

[3] Chatwin C., Farsari M., Huang S., Heywood M., Birch P., Young R., Richardson J., 1998, "UV Microstereolithography System That Uses Spatial Light Modulator Technology", *Applied Optics,* **37**(32), pp. 7514-22.

[4] Monneret S., Loubere V., Corbel S., 1999, "Microstereolithography Using Dynamic Mask Generator and A Non-Coherent Visible Light Source", *Proc. SPIE,* **3680**, pp. 553-561.

[5] Jariwala A., Ding F., Zhao X., Rosen D., 2009, "A Process Planning Method for Thin Film Mask Projection Micro- Stereolithography", Jariwala, A., Ding, F., Zhao, X., & Rosen, D. W., "A Process Planning Method for Thin Film Mask Projection Micro-Stereolithography", *Proceedings of the ASME 2009 International Design Engineering Technical Conferences & Computers and Information in Engineering Conference.* San Diego, CA, Paper no. DETC2009-87532, 2009.

[6] Referred website: http://envisiontec.com/products/perfactory-4-ddp/; visited on 15th July, 2013.

[7] Erdmann L., Deparnay A., Maschke G., Längle M., Bruner R., 2005, "MOEMS-Based Lithography for the Fabrication of Micro-Optical Components", *Journal of Microlithography, Microfabrication, Microsystems,* **4**(4), pp. 041601-1, -5.

[8] Mizukami Y., Rajnaik D., Rajnaik A., Nishimura M., 2002, "A Novel Microchip for Capillary Electrophoresis with Acrylic Microchannel Fabricated on Photosensor Array", *Sensors and Actuators B,* **81**, pp. 202-209.

[9] Jariwala A., Ding F., Zhao X., Rosen D., 2008, "A Film Fabrication Process on Transparent Substrate Using Mask Projection Stereolithography", D. Bourell, R. Crawford, C. Seepersad, J. Beaman, H. Marcus, eds., Proceedings of the 19th Solid Freeform Fabrication Symposium, Austin, Texas, pp. 216-229.

[10] Jariwala A., Ding F., Boddapati A., Breedveld V., Grover M. A., Henderson C. L., Rosen D. W., 2011, "Modeling effects of oxygen inhibition in mask-based Stereolithography", Rapid Prototyping Journal, 17(3), pp. 168-175.

[11] Jariwala A., Schwerzel R., Rosen D., 2011, "Real-Time Interferometric Monitoring System for Exposure Controlled Projection Lithography", Proceedings of the 22nd Solid Freeform Fabrication Symposium, Austin, Texas, pp. 99-10

[12] Referred website: http://www.cs.princeton.edu/courses/archive/fall06/cos576/papers/zetie_et_al_mach_zehnder00.pdf; visited 15th July, 2013.